Structure and Damping Properties of Polydimethylsiloxane and Polymethacrylate Sequential Interpenetrating Polymer Networks

GUANG-SU HUANG, QIANG LI, LU-XIA JIANG

Department of Polymer Science and Materials, Sichuan University, Chengdu Sichuan 610065, China

Received 19 March 2001; accepted 13 September 2001

ABSTRACT: By using the technology of the sequential interpenetrating polymer network, a series of novel damping materials based on a polydimethylsiloxane (PDMS)/polyacrylate (PAC) matrix with polymethacrylate (PMAC) were synthesized. They have a controllable broad transition peak spanning the temperature range of 150–220°C and the medial value of loss factor with maximum of 0.35–0.60. Dynamic mechanical analysis (DMA), differential scanning calorimetry (DSC), and atomic force microscopy (AFM) were applied to analyze and characterize the transition behavior and the microphase structure of the materials. It was found that the size and height of a transition peak at both the low- and the high-temperature zones change as a function not only of the concentration of PMAC and PDMS but also of the kind of PMAC; simultaneously, the low-temperature behavior was also governed by the crystallization of PDMS. The content of the crosslinking agent exerts a significant influence on the configuration of the curves of the transition peaks. AFM shows a characteristic phase morphology of double-phase continuity containing a transition layer and domain less than 1 μm, indicating that the interwoven multilayer networks are the key to incorporation of the immiscible components and form a broad damping functional region. © 2002 Wiley Periodicals, Inc. J Appl Polym Sci 85: 545–551, 2002

Key words: polysiloxane; polyacrylate; interpenetrating polymer networks; structure; properties

INTRODUCTION

An interpenetrating polymer network (INP) is defined as a combination of two polymers crosslinked by physical entanglement.[1] Given that the phase separation predicted by thermodynamics is restricted by the dynamic factor as interlocked dual networks, an IPN can incorporate two or multiple components with separation glass-transition temperatures (T_g's) and form a microheterogeneous structure, showing a much broader transition peak.

Near the T_g, under external force, the relaxation of polymer segments is characterized by a half-lagging condition to the external excitation, where the energy is dissipated as heat. Obviously, the wider the T_g transition region is, the broader the effective damping functional area will be. An example of the successful preparation of damping material from IPNs is polyurethane/vinyl polymer.[2–7]

Because polydimethylsiloxane (PDMS) is characterized by desirable properties (such as, for example, good thermal and oxidation stability, wa-

Correspondence to: G.-S. Huang.

Contract grant sponsor: Materials Division of National Science Foundation (China); contract grant number: 59873014.

Journal of Applied Polymer Science, Vol. 85, 545–551 (2002)

ter resistance, and chain flexibility), whereas polymethacrylate (PMAC) has a high $T_g\delta$ value in a relatively high temperature band and an abundance of applicable monomers whose polymers possess different T_g's, PDMS/PMAC IPNs have received considerable attention. In this respect, Sperling and Sarge[8] first synthesized the IPN of PDMS and PMMA by a sequential IPN. By using the system of room-temperature vulcanized silicone rubber, He and coinvestigators[9,10] developed an *in situ* sequential IPN method, in which dimethylsiloxane was first gelled followed by initiation of MMA. The essential characteristic of synthesis technology by Zhou et al.[11] lies in their introduction of a polyurethane crosslinking system in the first network of PDMS. All the abovementioned strategies are successful, by which a prominent reinforcing effect on PDMS can be obtained, with a concomitant improvement to toughness of PAC. However, there has been no comparable literature about damping materials prepared from PDMS and PMAC.

In this study we focus on the sequential IPNs of PMAC and PDMS based on a rubber matrix. Further, we report the encouraging initial research results and undertake to elucidate the relationship of factors, such as the composition of the materials, the effect of forced compatibility of the interwoven networks, the crystallization of PDMS, and the microphase structure of the IPNs, with the width and magnitude of the damping functional area.

EXPERIMENTAL

Materials

Polydimethylsiloxane (trade name MVQ 1102, supplied by Cheng Guang Chemistry Institute of China) has a weight-average molecular weight of 5×10^5 and a vinyl group content of 2.0 mol %. Polyacrylate (PAC) elastomer was obtained by emulsion polymerization in our laboratory (Mooney viscosity 50; iodine value $\sim$ 14). Alkyl methacrylate (MAC) monomers, such as methyl methacrylate (MMA), ethyl methacrylate (EMA), butyl methacrylate (nBMA), and the crosslinking agent of tripropyleneglycoldiacrylate (TPGDA) were freed from inhibitor by distilling under reduced pressure or by treating with column chromatography using neutral alumina.

Synthesis and Preparation of IPN Samples

Elastomers of PAC and PDMS were blended in a two-roll mill and 0. 8 phr of hexane peroxide was used as the crosslinking initiator. The blend of PDMS with PAC was vulcanized at 160–170°C under a pressure of about 5.0–10.0 MPa, which was used as the first network. Sequential IPNs were synthesized by swelling the first network with monomers such as MMA, EMA, or nBMA, containing 2.0, 3.0, and 3.0 wt % of TPGDA and 0.4 wt % of AIBN, respectively. The polymerization of the second network was conducted by compression molding at 70–90°C for a requisite time and then the samples were vacuum dried at 40°C to a constant weight.

Dynamic Mechanical Analysis (DMA)

A dynamic viscoelastometer 7E (Perkin Elmer Cetus Instruments, Norwalk, CT) was used to analyze and characterize the relaxation behavior of the macromolecular segments in the IPN samples under a heating rate of 1°C/min, a frequency of 1 Hz, and a compression or three-point bending mode.

Differential Scanning Calorimetry (DSC)

DSC (Du Pont 2910 DSC; Wilmington, DE) was used to measure the transition behavior of IPN samples. Before the measurement, both the temperature axis and the heat axis of the DSC instrument were calibrated with a series of standards and the samples were maintained 5 min after reaching -150°C. The measurement was conducted from -150 to 150°C with a scanning rate of 5°C/min.

Atomic Force Microscopy (AFM)

AFM (SII; Seiko Instruments, Japan) was used to characterize the microphase structure of the IPN samples. All images were collected in air using the tapping mode.

RESULTS AND DISCUSSION

Kind and Content of PMAC with Damping Behaviors

Figure 1 shows a series of semilogarithmic plots of the loss factors against temperature, in which a broad transition peak emerges for each curve ob-

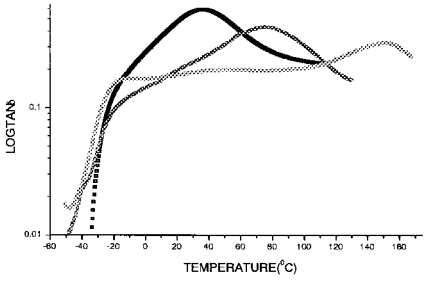

Figure 1 Plots of $T_g\delta$ versus temperature of IPNs based on PAC/PDMS with different PMACs: □, PnBMA; ○, PEMA containing 3.5 wt % TPGDA; △, PMMA.

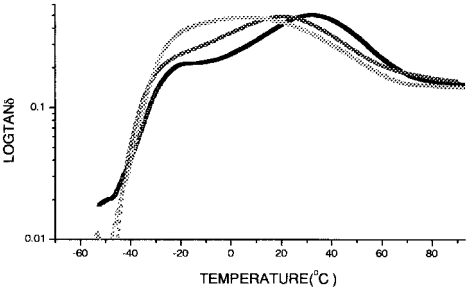

Figure 2 Plots of $T_g\delta$ versus temperature of IPNs based on PAC/PDMS with different contents of PnBMA: □, ~ 30%; ○, ~ 20%; △, ~ 10%.

tained from the IPNs of PDMS/PAC with PMMA, PEMA, and PnBMA, respectively. Table I shows their different components and data analysis of the DMA curves. However, the high-temperature position of the transition peaks is dominated by the kinds of PMAC serving as the second networks. For example, the peak shoulder representing PMMA appears at 150°C, where the shoulder of PnBMA emerges at 40°C, respectively representing the highest and the lowest temperature position in the high-temperature zone of the three glass-transition peaks. Reasonably, the high-temperature position involving PEMA is about 80°C. Another tendency, as shown in Figure 1 and Table I, is that with broadened glass transition toward higher temperature, the maximum value of the loss factors decreases from 0.60, to 0.45, and to 0.35 on the basis of the order of PnBMA, PEMA, and PMMA. Note that the glass-transition regions all exceed 100°C in width; the difference of the temperature position between PMMA and PnBMA can even exceed 100°C when the value of $T_g\delta_{max}$ decreases from 0.60 to 0.35, showing that the IPNs have as broad a transition range as could be expected based on its composition, although a decrease in the value of $T_g\delta_{max}$ is at the cost of widening. This phenomenon is readily attributable to the action of the different ester groups in PMAC. Methyl ester groups, because of their stiffness and volume effect, significantly retard the internal rotation of the main chain, causing the relaxation to slow and shifting the transition to high temperature. On the other hand, both ethyl ester and butyl ester groups have a relatively lower potential barrier, given that the side ester groups cause the distance between the molecules to increase, which can offset the volume effect of the bulky groups.[12]

As shown in Table I and Figure 2, the shoulders of PnBMA in transition peaks increase as the weight percentage rate of PnBMA increases from about 10 to 35%. Based on the same rate, there is an opposite tendency toward a decrease in the shoulders representing PAC/PDMS. Therefore,

Table I Influence of Types and Rates of PMAC on Damping Characteristics

		Temperature Range of T_g (°C)		
Composition (wt %)	$T_g\delta_{max}$	T_{onset}	T_{end}	ΔT
PDMS/PAC/PMMA				
37.0/37.0/26.0	0.35	−50	170	~220
PDMS/PAC/PEMA				
36.2/36.2/27.5	0.45	−50	120	~170
PDMS/PAC/PnBMA				
37.5/37.5/25.0	0.60	−35	120	~155
45.0/45.0/10.0	0.48	−49	53	~102
40.35/40.35/19.3	0.49	−45	60	~105
34.4/34.4/31.2	0.50	−50	65	~115

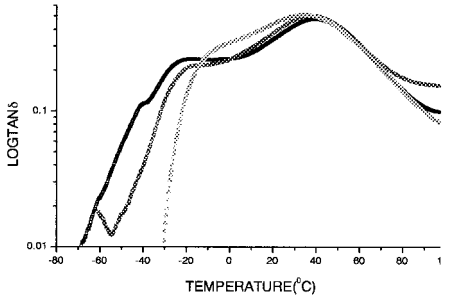

Figure 3 Plots of $T_g\delta$ versus temperature of the IPNs with different contents of PDMS: □, ~ 50%; ○, ~ 35%; △, ~ 21%.

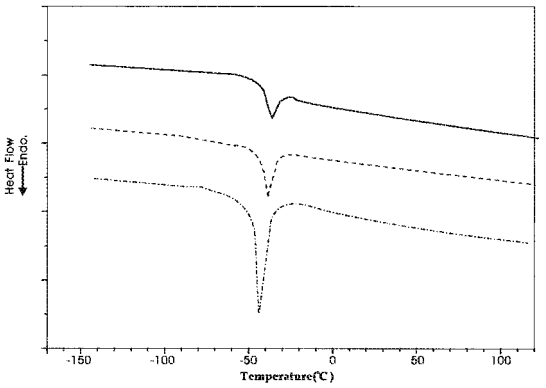

Figure 4 Plots of DSC of IPNs with different contents of PDMS: —, ~ 21%; - - -, ~ 35%; -·-·-, ~ 49%.

the sample containing 10% PnBMA has the highest peak at a low-temperature position, but the sample containing 35% PnBMA shows the highest value in the high-temperature zone, exhibiting a distinct change in the configuration of the transition peak curves. Besides, the peak of 10% PnBMA seems to be of greater compatibility than that of 35% PnBMA, given that the former has a narrower transition peak with a shoulder, whereas the latter has a relatively greater transition peak consisting of two shoulders.

Influence of the Content and Structure of PDMS on Damping Behavior

To determine the relationship between damping performances of the IPNs with PDMS content, a series of DMA experiments on samples with varying PDMS content was carried out. As exhibited in Figure 3 and Table II, with the increase of the PDMS the onset temperature of transition peak markedly shifts to lower temperatures: −69, −50, and −30°C, corresponding to about 50, 35, and 21% PDMS, respectively. However, the shoulders representing PDMS/PAC remain approximately constant, which results in expansion of the transition range. This phenomenon shows the typical low-temperature performances of PDMS to be exhibited in the low-temperature zone of the transition peak and suggests a combination between PDMS and PMAC attributed to either the nonbond coupling or the effect of forced compatibility. However, similar experiments still find that the result is not so ideal as expected; for example, there is always a lower $T_g\delta$ value at the low-temperature position in each transition peak.

Table II tabulates the analysis data from the plots of DMA. It indicates that with increases in the PDMS content, the width of the transition peak of the rubber and, accordingly, *TA* (defined as the area under the curve of $T_g\delta$ versus T) increases, but there is a concomitant decrease of *LA* (defined as the area under the curve of E'' versus T), which serves as a measurement of the additivity of the damping capability of the multicomponent materials. In general, the reason that PDMS causes *LA* to decrease and to contribute less toward the $T_g\delta$ value might be explained by the fact that the Si—O—Si has high flexibility and relatively large bond angle and bond length. Thus, PDMS exhibits a low potential barrier dur-

Table II Influence of Content of PDMS on Damping Characteristics

		Area		Temperature Range of T_g (°C)		
Composition (wt %)	$T_g\delta_{max}$	$T_g\delta \sim T$	$E'' \sim T$	T_{onset}	T_{end}	ΔT
PDMS/PAC/PnBMA						
49.7/21.3/29.0	0.47	37.95	1.08689×10^9	−69	70	139
35.5/35.5/28.1	0.50	36.64	1.30004×10^9	−50	70	120
21.3/48.9/28.7	0.52	34.95	1.55397×10^9	−30	70	100

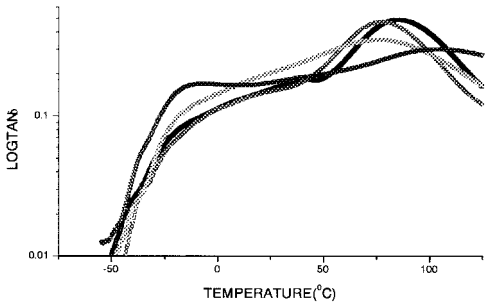

Figure 5 Plots of $T_g\delta$ versus temperature of the IPNs made with different contents of TPGDA: △, 0%; ▽, 2%; ○, 6%; □, 8%.

ing rotation.[13] Hence, as seen in Figure 4, the DSC plots of the corresponding samples reveal another factor, dominating the damping capability of PDMS at low temperature. As shown in Figure 4, a single melting peak appears at −45°C; moreover, the heat enthalpy change coincides with the concentration fluctuation of PDMS. The results demonstrate that the crystallization of PDMS,[14] equivalent to the elevating crosslinking degree, is a significant cause of the decrease in the E'' and $T_g\delta$ values, especially at the lower-temperature region. Because crystallization melting is the first transition, a glass transition is the second one. The former might cover or overlap the latter, which might be the reason that only one transition can be observed in the DSC plots.

Forced Compatibility and Phase Morphology

Although to date there is no direct evidence about the role of crosslinking agent in IPNs, it is universally acknowledged that forced compatibility, resulting from the crosslinking network, is the key to the successful preparation of IPNs.[2] Figure 5 and Table III show that from 0 to 8%, with the increase of crosslinking agent TPGDA, an obvious change takes place in the configuration of the curves of $T_g\delta$ versus T. When TPGDA is 0%, the transition peak consists of both shoulders representing PDMS/PAC and PEMA; however, with an elevated crosslinking agent concentration, at low temperatures the shoulders gradually diminish and approximate those of PEMA, forming a peak with only one shoulder. At the same time, the PEMA shoulders also slightly tend to higher temperature with increased TPGDA, which finally results in a peak splitting, when TPGDA reaches 8%. This is because increasing the crosslinking density decreases the domain size, thus creating more interface areas; furthermore, the interfacial mixing, compatibility, and the effect of nonbond coupling are enhanced, as both peaks of PDMS and PMAC are combined more intimately. Simultaneously, PEMA also gradually exhibits its independent behavior as the crosslinking agent concentration is increased.

Figure 6 shows the AFM micrographs of the samples. It is well known that TEM can distinguish phase morphology by straining one of the constituents. Recently, however, it has been realized that any difference in properties such as modulus, viscosity, friction force, and surface polarity can be used to discriminate the microphase structure of materials, provided that an apparatus could detect them. An AFM with tapping mode (TMAFM)[15–17] can do this, although it can observe only surface morphology. By using the principle that phase lag directly relates to the elastic modulus of materials, a TMAFM can be used to observe texture structures with multiple layers. In the system shown in Figure 6, the brighter domain might be PEMA or PnBMA because they have a relatively higher elastic modulus than that of other compositions. PDMS might

Table III Influence of Content of TPGDA on Damping Characteristics

Composition (wt %)	TPGDA (wt %)	$T_g\delta_{max}$	Temperature Range of T_g (°C)		
			T_{onset}	T_{end}	ΔT
PAC/PDMS/PEMA					
37.5/37.5/25.0	0	0.30	−50	130	180
37.5/37.5/25.0	2	0.35	−49	111	160
37.6/37.6/24.7	6	0.50	−44	108	152
36.9/36.9/26.2	8	0.54	−50	117	167

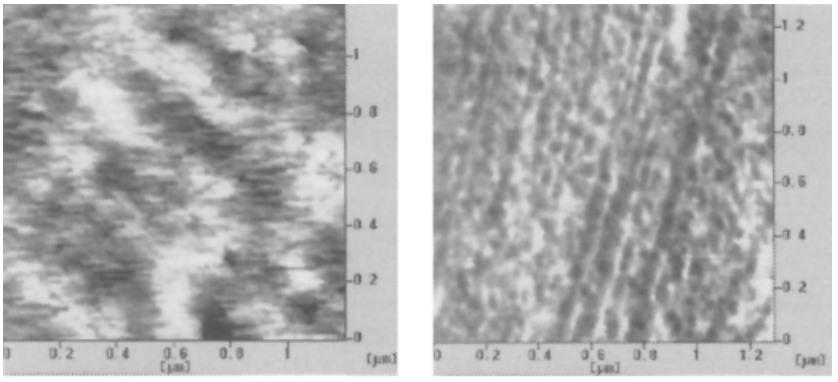

(a) (b)

Figure 6 AFM images: (a) sample containing ~ 50% PDMS, ~ 30% PnBA, and 3.5% TPGDA; (b) sample containing ~ 35% PDMS, ~ 25% PEMA, and 6.0% TPGDA.

be the darkest phase among them because of a relatively low elastic modulus at the ambient temperature. As displayed in the micrograph, the IPNs possess the structural characteristic of dual-phase continuity and the domain is less than 1 μm. Note that the two phases do not consist of only PEMA (or PnBMA) with PDMS. From the medial color band between the brighter and darker, PAC can be discriminated as a transition layer on the AMF micrograph. This confirms that PAC intertwined with PDMS in the PDMS/PAC matrix plays a mediating role to improve the compatibility; furthermore, the crosslinked PEMA, serving as the second network, intensifies the first network and causes the phase domain to become smaller. In other words, it is the effectiveness of forced compatibility from the multiple networks and the nonbond coupling from nearby groups that cause both immiscible phases to combine and to exhibit a single broad transition peak.

CONCLUSIONS

The transition peak of IPNs based on PDMS/PAC with PMAC was found to be dominated by PDMS at the lower-temperature zone but dominated by PMAC at the higher-temperature zone. These determining factors involve the content of both compositions, the kind of PMAC, and the crystallization of PDMS. The fluctuation of crosslinking agent concentration relates to the curve configuration of incorporation of two shoulders representing PDMS/PAC and PEMA. The single broad transition peak consists of two shoulders when the lower content of TPGDA is used, whereas a higher content of TPGDA causes both shoulders to combine, showing only one shoulder. The morphology characteristic of dual-phase continuity, containing a PAC transition layer and a phase domain of less than 1 μm, has been observed from TPAFM, indicating that forced compatibility, resulting from the multilayer network from IPNs and the PDMS/PAC covulcanized system, is the key to obtaining a broad damping functional region.

The authors gratefully acknowledge the Materials Division of National Science Foundation for financial support under Grant 59873014.

REFERENCES

1. Klempner, D.; Sperling, L. H. Interpenetrating Polymer Networks; ACS Books, Advances in Chemistry Series 239; American Chemical Society: Washington, DC, 1994.
2. Fay, J. J.; Murphy, C. T.; Tomas, D. A.; Sperling, L. H. Polym Eng Sci 1991, 31, 1731.
3. Chen, Q.; Hanhua, G. E. J Appl Polym Sci 1994, 54, 1191.
4. Chang, M. C. O.; Tomas, D. A.; Sperling, L. H. J Appl Polym Sci 1987, 34, 409.
5. Djomo, H.; Widmaier, J. M.; Meyer, G. C. Polymer 1983, 24, 65.
6. Djomo, H.; Windmaier, J. M.; Meyer, G. C. Polymer 1983, 24, 1415.
7. Hourston, D. J.; Schafer, F.-U. J Appl Polym Sci 1996, 62, 2025.
8. Sperling, L. H.; Sarge, H. D. J Appl Polym Sci 1972, 16, 3041.

9. He, X. W.; Widmaier, J. M.; Herz, J. E.; Meyer, G. C. Polymer 1992, 33, 866.
10. He, X. W.; Widmaier, J. M.; Herz, J. E.; Meyer, G. C. Polymer 1989, 30, 364.
11. Zhou, F.; Frisch, H. L.; Rogovina, L.; Sergeienko, N. J Polym Sci Part A: Polym Chem 1993, 31, 2481.
12. Hamurcu, E. E.; Baysal, B. M. Polymer 1993, 34, 5164.
13. Gong, Q. B.; Pan, X. G. Transition and Relaxation of Polymers; Chinese Science Publishing House: Beijing, 1986.
14. Liang, L. G. Polymer Chemistry in Silicone; Chinese Science Publishing House: Beijing, 1996.
15. Binnig, G.; Quate, C. F.; Cerber, Ch. Phys Rev Lett 1986, 56, 930.
16. Magonov, S. N.; Elings, V.; Whangbo, W. H. Surf Sci Lett 1997, 375, L385.
17. Tong, J. D.; Moineau, G.; Leclire, Ph. Macromolecules 2000, 33, 470.